Relativistic contributions to the deuteron electromagnetic form factors

G. Rupp
Centro de Física Nuclear, Instituto Nacional de Investigação Científica, P-1699 Lisboa Codex, Portugal

J. A. Tjon
Institute for Theoretical Physics, University of Utrecht, Princetonplein 5, NL-3508 TA Utrecht, The Netherlands
(Received 29 June 1989)

The deuteron electromagnetic form factors are calculated in the framework of the Bethe-Salpeter equation with multirank separable interactions. The only approximation made is the restriction to positive-energy states. A comparison is presented with the predictions of nonrelativistic, minimally relativistic, and other approximative calculations. The most important relativistic effect turns out to be the boost on the single-particle propagator due to recoil, in accordance with an earlier investigation.

I. INTRODUCTION

The electromagnetic (EM) form factors of the deuteron represent a fertile testing ground for nucleon-nucleon (NN) potentials, as well as for relativistic and non-nucleonic effects in the NN system. Especially since the recent measurements of the deuteron EM form factors at high momentum transfer[1,2] theoretical models are faced with the problem of explaining a host of accurate experimental data. However, the much less firmly established neutron form factors (see, e.g., Ref. 3) often provide models primarily based on nucleonic constituents with still sufficient room, so as not to be ruled out *a priori* by the deuteron data. It appears, therefore, important to try to reduce possible theoretical uncertainties to a minimum. In this spirit we propose to fix the magnitudes of the different relativistic contributions to the deuteron EM form factors within an albeit phenomenological yet by no means unrealistic model calculation. In an earlier article,[4] hereafter referred to as ZT, Zuilhof and Tjon already carried out a similar investigation in the framework of the Bethe-Salpeter (BS) equation for two spin-$\frac{1}{2}$ particles interacting through one-boson-exchange (OBE) potentials. Due to the complexity of the problem, however, a few approximations had to be made with respect to the exact expressions, thereby leaving some doubt about the accuracy of the predictions. Furthermore, a direct and straightforward comparison with a nonrelativistic (NR) calculation was not very meaningful. Thus, in this paper we employ relativistically covariant, separable potentials in the context of the BS equation for two Dirac particles, which allow a rigorous relativistic calculation, including recoil effects. The interactions we choose, being very similar to those employed in a Faddeev-type Bethe-Salpeter calculation of trinucleon observables,[5] are covariant generalizations of the NR separable Graz-II potential,[6] with refitted coupling strengths, so as to reproduce the $^3S_1$ and $^3D_1$ NN scattering data and the static deuteron properties with the same precision as the original NR potential. This also permits us to make a sound comparison with the NR predictions, apart from an extensive study of the various relativistic effects. Here we note that, for simplicity, we disregard negative-energy states in our calculations, which approximation is fully justified by the conclusion in ZT that their influence is negligible up to moderately high momentum transfers.

This paper is set up as follows: In Sec. II the BS equation for multirank separable potentials is solved and the results of fits to the NN data with different values of the D-state probability are presented. Section III is a resume of the derivation of the deuteron EM form factors in terms of the BS wave function for a bound state of two Dirac particles. In Sec. IV the various EM form factors are presented and compared, not only with the respective NR curves, but also with the predictions of several approximative calculations, so as to find out what are the relative magnitudes of the different relativistic effects. Section V, finally, contains a summary of the principal results and some conclusions.

II. BS EQUATION WITH SEPARABLE INTERACTIONS

In momentum space, the BS equation for the T matrix describing relativistic two-particle scattering reads, in terms of the relative four-momenta p, p', k, and the center-of-mass (c.m.) energy squared s,

$$T(p,p';s)=V(p,p')+\frac{i}{4\pi^3}\int d^4k\; V(p,k)S(k;s)T(k,p';s)\;, \tag{1}$$

where $V(p,p')$, in principle, stands for the set of all irreducible diagrams, and $S(k;s)$ is the free two-particle Green's

TABLE I. Parameters of original Graz-II potential.

β_{11}	$2.313\,84\times10^{-1}$ GeV	λ_{11}	$3.105\,80\times10^{-3}$ GeV^8
β_{12}	$5.217\,05\times10^{-1}$ GeV	λ_{12}	$-5.546\,63\times10^{-1}$ GeV^6
β_{21}	$7.949\,07\times10^{-1}$ GeV	λ_{13}	$-2.017\,38\times10^{-2}$ GeV^8
β_{22}	$1.575\,12\times10^{-1}$ GeV	λ_{22}	108.0 88 GeV^4
γ_1	28.695 5 GeV^2	λ_{23}	2.727 01 GeV^6
γ_2	64.98 03 GeV^2	λ_{33}	$2.986\,50\times10^{-2}$ GeV^8

function. If we consider two equal-mass spin-$\frac{1}{2}$ particles in the coupled-triplet case and neglect negative-energy states (see also Secs. III and IV), we obtain the partial-wave-decomposed equations

$$T_{LL'}(p_0,|\mathbf{p}|;p_0',|\mathbf{p}'|;s)=V_{LL'}(p_0,|\mathbf{p}|;p_0',|\mathbf{p}'|)+\frac{i}{2\pi^2}\sum_{L''=0,2}\int dk_0\int|\mathbf{k}^2|d|\mathbf{k}|\;V_{LL''}(p_0,|\mathbf{p}|;k_0,|\mathbf{k}|)S(k_0,|\mathbf{k}|;s)T_{L''L'}(k_0,|\mathbf{k}|;p_0',|\mathbf{p}'|;s)\;, \tag{2}$$

where $S(k_0,|\mathbf{k}|;s)=\{(\frac{1}{2}\sqrt{s}-E_k)^2-k_0^2\}^{-1}$, with $E_k=(\mathbf{k}^2+m^2)^{1/2}$. The fully on-shell T matrix, defined by $T_{LL'}(|\bar{\mathbf{p}}|)\equiv T_{LL'}(\bar{p}_0,|\bar{\mathbf{p}}|;\bar{p}_0,|\bar{\mathbf{p}}|;s)$, with $\bar{p}_0=0$ and $|\bar{\mathbf{p}}|=(\frac{1}{4}s-m^2)^{1/2}=(\frac{1}{2}mE_{\text{lab}})^{1/2}$, is related to the $^3S_1$ and $^3D_1$ scattering phase shifts as

$$T_{LL}(|\bar{\mathbf{p}}|)=-\frac{4\sqrt{s}}{|\bar{\mathbf{p}}|}e^{i\delta_L(|\bar{\mathbf{p}}|)}\sin\delta_L(|\bar{\mathbf{p}}|)\;. \tag{3}$$

If we now choose for the interaction V a rank-N separable ansatz of the form

$$V_{LL'}(p,p')=\sum_{i,j=1}^{N}\lambda_{ij}g_i^{(L)}(p^2)g_j^{(L')}(p'^2)\;, \tag{4}$$

the BS equation can be solved in closed form. The result for the T matrix is

$$T_{LL'}(p_0,|\mathbf{p}|;p_0',|\mathbf{p}'|;s)=\sum_{i,j=1}^{N}\tau_{ij}(s)g_i^{(L)}(p^2)g_j^{(L')}(p'^2)\;, \tag{5}$$

with

$$[\tau^{-1}(s)]_{ij}=[\lambda^{-1}]_{ij}-\frac{i}{2\pi^2}\sum_{L'=0,2}\int_{-\infty}^{\infty}dk_0\int_0^{\infty}|\mathbf{k}^2|d|\mathbf{k}|\;S(k_0,|\mathbf{k}|;s)g_i^{(L')}(k^2)g_j^{(L')}(k^2)\;. \tag{6}$$

Similarly, the bound-state (deuteron) wave function becomes

$$\psi_L(p_0,|\mathbf{p}|)=S(p_0,|\mathbf{p}|;s)\phi_L(p_0,|\mathbf{p}|)\;, \tag{7}$$

with $s=m_d^2$, and where the deuteron vertex function ϕ is given by

$$\phi_L(p_0,|\mathbf{p}|)=\sum_{i,j=1}^{N}\lambda_{ij}g_i^{(L)}(p_0,|\mathbf{p}|)c_j(s)\;. \tag{8}$$

TABLE II. Refitted couplings of Graz-II-type interactions.

P_D		λ_{11}[a]	λ_{12}[b]	λ_{13}[a]	λ_{22}[c]	λ_{23}[b]	λ_{33}[a]
4%	NR	$3.357\,24\times10^{-3}$	$-7.808\,89\times10^{-1}$	$-2.254\,84\times10^{-2}$	170.283	3.426 10	$4.052\,94\times10^{-2}$
	BSLT	$3.937\,60\times10^{-4}$	$-3.468\,36\times10^{-1}$	$-1.672\,42\times10^{-2}$	104.769	2.399 46	$2.491\,97\times10^{-2}$
	BS	$6.024\,23\times10^{-3}$	$-1.588\,04$	$-3.362\,12\times10^{-2}$	366.114	6.338 06	$7.723\,54\times10^{-2}$
5%	NR	$3.050\,65\times10^{-3}$	$-5.082\,87\times10^{-1}$	$-1.968\,67\times10^{-2}$	96.0983	2.592 44	$2.782\,35\times10^{-2}$
	BSLT	$5.873\,84\times10^{-4}$	$-1.953\,77\times10^{-1}$	$-1.601\,01\times10^{-2}$	57.9262	1.985 53	$1.834\,08\times10^{-2}$
	BS	$2.360\,62\times10^{-4}$	$-3.365\,32\times10^{-2}$	$-1.426\,08\times10^{-2}$	20.3917	1.655 93	$1.440\,02\times10^{-2}$
6%	NR	$2.964\,42\times10^{-3}$	$-2.987\,33\times10^{-1}$	$-1.755\,66\times10^{-2}$	41.9506	2.006 21	$1.867\,86\times10^{-2}$
	BSLT	$9.374\,41\times10^{-4}$	$-8.327\,04\times10^{-2}$	$-1.561\,66\times10^{-2}$	22.5999	1.713 46	$1.353\,30\times10^{-2}$
	BS	$5.851\,81\times10^{-4}$	$1.824\,42\times10^{-1}$	$-1.306\,11\times10^{-2}$	-26.6096	1.093 45	$7.165\,63\times10^{-3}$

[a]In GeV^8.
[b]In GeV^6.
[c]In GeV^4.

TABLE III. Deuteron properties and low-energy $^3S_1$ scattering parameters.

		a (fm)	r_0 (fm)	B_d (MeV)	Q_d (fm^2)	μ_d $\left[\frac{e}{2m_N}\right]$	$\rho_{D/S}$
$P_D=4\%$	NR	5.418	1.780	2.2254	0.2575	0.8572	0.025 00
	BSLT	5.419	1.779	2.2254	0.2664	0.8572	0.025 92
	BS	5.419	1.781	2.2254	0.2499	0.8568	0.024 08
$P_D=5\%$	NR	5.419	1.780	2.2254	0.2859	0.8515	0.027 94
	BSLT	5.420	1.779	2.2254	0.2957	0.8515	0.028 96
	BS	5.420	1.779	2.2254	0.2774	0.8512	0.026 90
$P_D=6\%$	NR	5.420	1.779	2.2254	0.3112	0.8458	0.030 59
	BSLT	5.421	1.778	2.2254	0.3217	0.8458	0.031 71
	BS	5.421	1.778	2.2254	0.3019	0.8458	0.029 45
$P_D=4.82\%$	Graz-II	5.419	1.780	2.2254	0.2812	0.8525	0.027 45
Experiment		5.424	1.759	2.2246	0.286	0.8574	0.0263

Here, the coefficients $c_j(s)$ are determined, up to an overall normalization, by the homogeneous set of N algebraic equations

$$c_j(s)-\sum_{k,l=1}^{N} H_{jk}(s)\lambda_{kl}c_l(s)=0 , \tag{9}$$

where the matrix H is defined by

$$H_{jk}(s)=\frac{i}{2\pi^2}\sum_{L'=0,2}\int_{-\infty}^{\infty}dk_0\int_0^{\infty}|\mathbf{k}|^2d|\mathbf{k}|\,S(k_0,|\mathbf{k}|;s)g_j^{(L')}(k_0,|\mathbf{k}|)g_k^{(L')}(k_0,|\mathbf{k}|) . \tag{10}$$

In this investigation we use a relativistically covariant generalization of the NR separable Graz-II potential[6] in order to describe the NN system in the coupled $^3S_1$ and $^3D_1$ waves, being of rank three in this specific case. The employed form factors are

$$\begin{aligned} g_1^{(0)}&=\frac{1-\gamma_1p^2}{(p^2-\beta_{11}^2)^2},\; g_2^{(0)}=-\frac{p^2}{(p^2-\beta_{12}^2)^2} ,\\ g_3^{(2)}&=\frac{p^2(1-\gamma_2p^2)}{(p^2-\beta_{21}^2)(p^2-\beta_{22}^2)^2},\; g_1^{(2)}=g_2^{(2)}=g_3^{(0)}\equiv 0 . \end{aligned} \tag{11}$$

The parameters β_{ab} and γ_a are left unaltered with respect to the original potential (see Table I), while the λ_{ij} are refitted, also in the NR case, in order to reproduce, for three different values of the D-state probability P_D (4%, 5%, 6%), as well as possible the $^3S_1$ and $^3D_1$ NN scattering phase shifts up to a laboratory energy of 500 MeV, the scattering length a and the effective range r_0, and the static deuteron properties, viz., the binding energy B_d, the quadrupole moment Q_d, the magnetic moment μ_d, and the asymptotic D/S-state ratio $\rho_{D/S}$. This is repeated employing the BSLT (Ref. 7) approximation, for scalar particles, to the BS equation (for details, see, e.g., Ref. 8, Sec. II), however, without changing the form factors, so that it does not become equivalent to the NR case, contrary to the approach in Ref. 8. Thus we get nine sets of refitted couplings, given in Table II. The resulting deuteron properties and low-energy scattering parameters are presented in Table III, together with the original Graz-II predictions and the experimental values. The calculated $^3S_1$ and $^3D_1$ phase shifts, though not depicted, are very similar to the ones obtained with the original potential. From Table III we see that, for the type of interactions used, the best agreement with experiment is obtained with a D-state probability of about 5%.

III. DEUTERON ELECTROMAGNETIC FORM FACTORS

Here we sketch the derivation of the expressions for the deuteron electromagnetic form factors in terms of the bound-state BS wave function. A more complete treatment can be found in ZT.

In the limit of vanishing electron mass, the differential cross section for elastic electron-deuteron scattering can be expressed in terms of the Mott cross section and the charge, quadrupole, and magnetic form factors of the deuteron as

$$d\sigma=d\sigma_{\text{Mott}}\left[A(q^2)+B(q^2)\tan^2\frac{\theta}{2}\right] , \tag{12}$$

where

$$\begin{aligned} A(q^2)&=F_C^2+\tfrac{8}{9}\eta^2F_Q^2+\tfrac{2}{3}\eta F_M^2 ,\\ B(q^2)&=\tfrac{4}{3}\eta(1+\eta)F_M^2 , \end{aligned} \tag{13}$$

with $\eta=-(q^2/2m_d)$. These form factors are normalized at zero momentum transfer as $F_C(0)=1$, $F_Q(0)=m_d^2Q_d$, and $F_M(0)=(m_d/m_N)\mu_d$, where m_d, Q_d, and μ_d are, respectively, the deuteron mass, quadrupole moment, and magnetic moment, and where m_N is the (average) nucleon mass. Note that from unpolarized scattering data only the quantities A and B can be extracted, so not F_C and F_Q separately. In the one-photon-exchange approximation, the amplitude for the above scattering process is just the contraction of the electron and deuteron currents, multiplied by the photon propagator, i.e.,

$$\langle k',\lambda'|j^e_\mu|k,\lambda\rangle \frac{1}{q^2}\langle P',M'|J^\mu_d|P,M\rangle \ , \tag{14}$$

where $\langle k',\lambda'|j^e_\mu|k,\lambda\rangle = ie\bar{u}_{\lambda'}(\mathbf{k}')\gamma_\mu u_\lambda(\mathbf{k})$. From Lorentz covariance and time-reversal invariance one infers that the deuteron current can be written as

$$\langle P',M'|J^\mu_d|P,M\rangle = -\frac{e}{2m_d} e^{*\rho}(\mathbf{P}',M')J^\mu_{\rho\sigma}e^\sigma(\mathbf{P},M) \ , \tag{15}$$

where the spin-1 polarization vectors e^μ satisfy the properties

$$\begin{aligned} &e^*_\mu(\mathbf{P},M)e^\mu(\mathbf{P},M') = -\delta_{MM'} \ , \\ &\sum_M e^*_\mu(\mathbf{P},M)e_\nu(\mathbf{P},M) = -g_{\mu\nu} + \frac{P_\mu P_\nu}{m_d^2} \ , \\ &P_\mu e^\mu(\mathbf{P},M) = 0 \ , \end{aligned} \tag{16}$$

and where the operator $J^\mu_{\rho\sigma}$ is given by

$$J^\mu_{\rho\sigma} = (P'_\mu + P_\mu)\left[g_{\rho\sigma}F_1(q^2) - \frac{q_\rho q_\sigma}{2m_d^2}F_2(q^2)\right] + I^{\mu\nu}_{\rho\sigma}q_\nu G_1(q^2) \ . \tag{17}$$

Here, $I^{\mu\nu}_{\rho\sigma}$ is the generator of infinitesimal Lorentz transformations, and F_1, F_2, G_1 are invariant functions of q^2. The latter are related to the deuteron charge, quadrupole, and magnetic form factors as

$$\begin{aligned} &F_C = F_1 + \tfrac{2}{3}\eta[F_1 + (1+\eta)F_2 + G_1] \ , \\ &F_Q = F_1 + (1+\eta)F_2 + G_1 \ , \\ &F_M = G_1 \ . \end{aligned} \tag{18}$$

Hence, we see from Eqs. (15)–(18) that the so-defined deuteron current meets the normalization condition

$$\lim_{q^2\to 0}\langle P',M'|J^\mu_d|P,M\rangle = e\frac{P^\mu}{m_d}\delta_{M'M} \ . \tag{19}$$

Choosing now the *Breit* frame, defined by $\mathbf{P}'=\mathbf{P}+\mathbf{q}=-\mathbf{P}$, i.e., $\mathbf{P}=-\frac{1}{2}\mathbf{q}$ and $q^0=0$, and taking the photon momentum along the z axis, we arrive at the expressions (suppressing the references to the, now fixed, total momenta P and P')

$$\begin{aligned} \langle M'|J^0_d|M\rangle &= e\sqrt{1+\eta}\{F_1\delta_{MM'} + 2\eta[F_1 + (1+\eta)F_2 + G_1]\delta_{M'0}\delta_{M0}\} \ , \\ \langle M'|J^x_d|M\rangle &= \frac{e}{\sqrt{2}}\sqrt{\eta}\sqrt{1+\eta}G_1[\delta_{M',M+1} - \delta_{M',M-1}] \ , \\ \langle M'|J^y_d|M\rangle &= -i\frac{e}{\sqrt{2}}\sqrt{\eta}\sqrt{1+\eta}G_1[\delta_{M',M+1} + \delta_{M',M-1}] \ , \\ \langle M'|J^z_d|M\rangle &= 0 \ . \end{aligned} \tag{20}$$

Now we are going to express the deuteron current in terms of a general solution of the bound-state BS equation. Near the deuteron pole, the T matrix takes the separable form

$$T(p',p;P) = \sum_M \frac{\phi^{(M)}(p';P)\tilde{\phi}^{(M)}(p;P)}{P^2 - m_d^2} \ , \tag{21}$$

where the deuteron vertex functions ϕ and $\tilde{\phi}$ satisfy the homogeneous BS equation, with the normalization condition

$$2P_\mu\delta_{M'M} = \frac{i}{4\pi^3}\int d^4p\, \tilde{\phi}^{(M')}(p;P)\left[\frac{\partial}{\partial P^\mu}S(p;P)\right]\Bigg|_{P^2=m_d^2} \times \phi^{(M)}(p;P) \ , \tag{22}$$

if we assume that the interactions are independent of the total momentum P. In the impulse approximation, the deuteron current can then be expressed as

$$\begin{aligned} \langle P',M'|J^d_\mu|P,M\rangle = \frac{ie}{16\pi^3 m_d}\int d^4p[&\tilde{\phi}^{(M')}(p';P')S^{(1)}(p';P')\Gamma^{(1)}_\mu(q)S(p,P)\phi^{(M)}(p;P) \\ &+ \tilde{\phi}^{(M')}(p'';P')S^{(2)}(p'';P')\Gamma^{(2)}_\mu(q)S(p;P)\phi^{(M)}(p;P)] \ , \end{aligned} \tag{23}$$

with $p'=p+\frac{1}{2}q$, $p''=p-\frac{1}{2}q$, $P'=P+q$, and where the two-particle Dirac propagator $S(p;P) \equiv S^{(1)}(p;P)S^{(2)}(p;P)$ reads

$$S(p;P) = (\tfrac{1}{2}\not{P}^{(1)} + \not{p}^{(1)} - m_N)^{-1}(\tfrac{1}{2}\not{P}^{(2)} - \not{p}^{(2)} - m_N)^{-1} \ . \tag{24}$$

Here, the superscripts indicate that the contracted gamma matrices act on the spinors of the respective particles only. The EM photon-nucleon vertex operator Γ_μ in Eq. (23) is assumed to be of the on-shell form

$$\Gamma_\mu(q) = \gamma_\mu F^{(N)}_1(q^2) - \frac{1}{2m_N}\sigma_{\mu\nu}q^\nu F^{(N)}_2(q^2) \ , \tag{25}$$

where $\sigma_{\mu\nu} = \frac{i}{2}[\gamma_\mu, \gamma_\nu]$. Note that, since the deuteron has isospin $I=0$, only the isoscalar components of the nucleon form factors $F^{(N)}_1$ and $F^{(N)}_2$ are needed. Using the identity

$$\frac{\partial}{\partial P^\mu}S(p;P) = \tfrac{1}{2}[S^{(1)}(p;P)\gamma^{(1)}_\mu S(p;P) + S^{(2)}(p;P)\gamma^{(2)}_\mu S(p;P)] \ , \tag{26}$$

we conclude from Eq. (25) that the above-defined deuteron current straightforwardly satisfies the normalization condition (22). Also, due to invariance of the BS equation under the interchange of particles 1 and 2, the second term on the right-hand side of Eq. (23) is equal to the first one. Moreover, the isoscalar current is manifestly gauge invariant for the BS equation in ladder approximation, as well as in a covariant separable representation. The former case is proved in ZT, the latter in the present Appendix A.

Now we proceed to transform Eq. (23), being valid in any Lorentz frame, to the CM frame, in which the bound-state BS equation has been solved. Thereto we make use of the general transformation rules

$$\begin{aligned}
&\phi^{(M)}(p;P)=\Lambda^{(1)}(\mathcal{L})\Lambda^{(2)}(\mathcal{L})\phi^{(M)}(\mathcal{L}^{-1}p;\mathcal{L}^{-1}P)\ ,\\
&\bar{\phi}^{(M)}(p;P)=\bar{\phi}^{(M)}(\mathcal{L}^{-1}p;\mathcal{L}^{-1}P)\Lambda^{(1)^{-1}}(\mathcal{L})\Lambda^{(2)^{-1}}(\mathcal{L})\ ,\\
&S^{(i)}(p;P)=\Lambda^{(i)}(\mathcal{L})S^{(i)}(\mathcal{L}^{-1}p;\mathcal{L}^{-1}P)\Lambda^{(i)^{-1}}(\mathcal{L})\ ,\\
&V(p,p')=\Lambda^{(1)}(\mathcal{L})\Lambda^{(2)}(\mathcal{L})V(\mathcal{L}^{-1}p,\mathcal{L}^{-1}p')\Lambda^{(1)^{-1}}(\mathcal{L})\\
&\qquad\times\Lambda^{(2)^{-1}}(\mathcal{L})\ .
\end{aligned} \tag{27}$$

Here, $\Lambda^{(i)}(\mathcal{L})$ is the Dirac operator for particle i, corresponding to the Lorentz transformation $\mathcal{L}$. With these transformation laws, the BS equation is clearly covariant. In the sequel, only boosts along the z axis are needed, given by (dropping the particle index)

$$\Lambda(\mathcal{L})=\left[\frac{E_d+m_d}{2m_d}\right]^{1/2}\left[1+\gamma^0\gamma^3\frac{|\mathbf{P}|}{E_d+m_d}\right]\ , \tag{28}$$

with $|\mathbf{P}|$ the boost momentum and $E_d=(\mathbf{P}^2+m_d^2)^{1/2}$.

Since the expressions (20) for the matrix elements of the deuteron current were obtained in the Breit frame, with the photon along the z axis, we now use the same starting point to evaluate Eq. (23). Then, we have the relations (cf. Ref. 8)

$$\begin{aligned}
&P_{\text{c.m.}}=\mathcal{L}^{-1}P_B;\ p_{\text{c.m.}}=\mathcal{L}^{-1}p_B;\ P'_{\text{c.m.}}=\mathcal{L}P'_B\ ,\\
&p'_{\text{c.m.}}=\mathcal{L}p'_B=\mathcal{L}(p_B+\tfrac{1}{2}q_B)=\mathcal{L}[\mathcal{L}p_{\text{c.m.}}+\tfrac{1}{2}(0,0,0,|\mathbf{q}|)]\ ,
\end{aligned} \tag{29}$$

where the subscripts refer to the respective frames. The explicit form of the boost $\mathcal{L}$ is given in ZT and Ref. 8. Hence, employing the transformation laws (27), applied to $\mathcal{L}^{-1}$ in the case of primed momenta, and the invariance of the four-volume element, i.e., $d^4p_B=d^4(\mathcal{L}p_{\text{c.m.}})=d^4p_{\text{c.m.}}$, we arrive at an expression in terms of CM vertex functions and propagators, reading

$$\langle P',M'|J_\mu^d|P,M\rangle=\frac{ie}{8\pi^3m_d}\int d^4k\,\bar{\phi}^{(M')}(k';P_{\text{c.m.}})S^{(1)}(k';P_{\text{c.m.}})\tilde{\Gamma}_\mu^{(1)}(q)S(k;P_{\text{c.m.}})\phi^{(M)}(k;P_{\text{c.m.}})\ , \tag{30}$$

with $k\equiv p_{\text{c.m.}}$, $k'\equiv p'_{\text{c.m.}}$, and

$$\tilde{\Gamma}_\mu^{(1)}(q)\equiv\Lambda^{(1)}(\mathcal{L})\Lambda^{(2)}(\mathcal{L})\Gamma_\mu^{(1)}(q)\Lambda^{(1)}(\mathcal{L})\Lambda^{(2)}(\mathcal{L})=\Lambda^{(1)}(\mathcal{L})\Gamma_\mu^{(1)}(q)\Lambda^{(1)}(\mathcal{L})[\Lambda^{(2)}\mathcal{L})]^2\ .$$

Next the partial-wave decomposition has to be carried out. Since in ZT this has been done in great detail, here only the final result will be presented. On a basis of two-particle helicity states, which are orthogonal and form a complete set, the two-nucleon system is, in principle, represented by a set of 16 coupled channels, accounting for the positive- and negative-energy states of both particles, and for their spin degrees of freedom. For a coupled-triplet state with definite parity, this number reduces to eight, which channels are most conveniently described on a basis labeled by total J, L, S, and ρ, the so-called energy spin. Energy spin up or down for either particle means that it is in a positive- or negative-energy state, respectively. Thus, we obtain eight channels, spectroscopically denoted by ${}^{2S+1}L_J^\rho$, reading

$$\begin{aligned}
&(1)\ {}^3S_1^+,\ (2)\ {}^3D_1^+,\ (3)\ {}^3S_1^-,\ (4)\ {}^3D_1^-\ ,\\
&(5)\ {}^1P_1^e,\ (6)\ {}^3P_1^o,\ (7)\ {}^1P_1^o,\ (8)\ {}^3P_1^e\ ,
\end{aligned} \tag{31}$$

where e and o stand for even and odd, respectively, combinations of antiparallel single-particle ρ spins. The corresponding eight-component vertex function is denoted by $\phi_n(p_0,\mathbf{p})$. Its conjugate differs by a phase factor only, which we choose to be -1. Thus, we arrive at the following expression for the deuteron current:

$$\begin{aligned}
\langle P',M'|J_\mu^d|P,M\rangle=\frac{-ie}{8\pi^2m_d}\sum_{\substack{n_1n_2\\n_3n_4}}^{8}\int_{-\infty}^{\infty}dk_0\int_0^\infty|\mathbf{k}^2|d|\mathbf{k}|\int_{-1}^{1}d\cos\theta\,\phi_{n_1}(k'_0,|\mathbf{k}'|)S_{n_1n_2}^{(1)}(k'_0,|\mathbf{k}'|)\tilde{\Gamma}_{\mu,n_2n_3}^{(1)}(\mathbf{k}',\mathbf{k};q)\\
\times S_{n_3n_4}(k_0,|\mathbf{k}|)\phi_{n_4}(k_0,|\mathbf{k}|)\ ,
\end{aligned} \tag{32}$$

where

$$\begin{aligned}
\tilde{\Gamma}_{\mu,n_2n_3}^{(1)}(\mathbf{k}',\mathbf{k};q)=\tfrac{1}{2}\sqrt{(2L'+1)(2L+1)}\\
\times\sum_{\substack{\lambda'_1\lambda'_2\\\lambda_1\lambda_2}}[D_{M'\lambda'}^{(1)}(\Omega_{\mathbf{k}'})C_{0\lambda'\lambda'}^{L'S'J}C_{\lambda'_1-\lambda'_2\lambda'}^{\frac{1}{2}\frac{1}{2}S'}\bar{V}_{\lambda'_1}^{\rho'_1}(\mathbf{k}')V_{\lambda'_2}^{\rho_2'^{\dagger}}(\mathbf{k}')\hat{\Gamma}_\mu^{(1)}(q)V_{\lambda_1}^{\rho_1}(\mathbf{k})V_{\lambda_2}^{\rho_2}(\mathbf{k})C_{0\lambda\lambda}^{LSJ}C_{\lambda_1-\lambda_2\lambda}^{\frac{1}{2}\frac{1}{2}S}D_{M\lambda}^{(1)*}(\Omega_{\mathbf{k}})]\ .
\end{aligned} \tag{33}$$

Here, $V_{\lambda_i}^{\rho_i}$ stands for the helicity spinor of particle i, and

$$\hat{\Gamma}_\mu^{(1)}(q) \equiv \Lambda^{(1)}(\mathcal{L})\Gamma_\mu^{(1)}(q) f_{M'M}\Lambda^{(1)}(\mathcal{L})[\Lambda^{(2)}(\mathcal{L})]^2 ,$$

with

$$f_{M'M} = \begin{cases} \delta_{M'M} & \text{for } \mu=0,3 \\ \frac{1}{2}[(\delta_{M',M+1}+\delta_{M',M-1})-i\gamma^1\gamma^2(\delta_{M',M+1}-\delta_{M',M-1})] & \text{for } \mu=1,2 . \end{cases} \tag{34}$$

The matrix elements of $\tilde{\Gamma}$ are evaluated with the algebraic program REDUCE. First, the boosted EM operator $\hat{\Gamma}$ is computed on the helicity basis, giving rise to, in principle, 256 separate terms, for each μ. If we neglect negative-energy states, i.e., choose all ρ's positive, this number reduces to 16, of which only 4 are different, due to symmetry properties (see Appendix B for the explicit expressions). Next the change to the spectroscopic basis is made, given by Eq. (33). Finally, μ, M', and M are chosen such that the invariant functions F_1, F_2, G_1, and thus the form factors F_C, F_Q, F_M, can be read off from the general expressions (20) and (18). In fact, it is sufficient to compute the current matrix elements $\langle 0|J_d^0|0\rangle$, $\langle 1|J_d^0|1\rangle$, and $\langle 1|J_d^1|0\rangle$. What then remains to be done is a three-dimensional numerical integration over p_0, $|\mathbf{p}|$, and $\cos\theta$, the former of which requires special precautions because of the complicated singularity structure of the integrand. This will be discussed in Sec. IV.

IV. RESULTS AND DISCUSSION

The propagators and vertex functions in Eq. (32) have singularities in the complex k_0 plane, infinitesimally close to the real axis, which complicate a numerical evaluation. In the case of separable interactions, all of these are simple poles, so that, in principle, the k_0 integration can be carried out analytically, applying Cauchy's theorem. An alternative, employed here, is to perform a Wick rotation in this variable, thereby accounting for only those poles that are encountered in the rotation process. The only reason for the latter choice is to have a more straightforward comparison with the calculation done in ZT, where the first option was not feasible due to the branch-cut singularities of the vertex function for an OBE model. Thus, we have to study the behavior of the various poles of the integrand. The ones corresponding to the initial state always remain in the same quadrant, viz, the second or the fourth, whence they do not affect the Wick rotation. Explicitly, the poles of the two-particle propagator are located at $k_0 = \pm\frac{1}{2}m_d - (\mathbf{k}^2+m_N^2)^{1/2}+i\epsilon$ and $k_0 = \pm\frac{1}{2}m_d + (\mathbf{k}^2+m_N^2)^{1/2}-i\epsilon$, respectively, and the ones of the vertex function at $-(\mathbf{k}^2+\beta_{ab}^2)^{1/2}+i\epsilon$ and $(\mathbf{k}^2+\beta_{ab}^2)^{1/2}-i\epsilon$, respectively, where $a,b=1,1$ or $a,b=1,2$, for the $^3S_1$ channel, and $a,b=2,1$ or $a,b=2,2$ for the $^3D_1$. Owing to the boost transformations, the singularities in the final state are more intricate. The single-particle propagator has poles at

$$k_0 = -\tfrac{1}{2}(1+4\eta)m_d \pm [(\mathbf{k}^2+m_N^2+2\alpha m_d|\mathbf{k}|\cos\theta + \alpha^2 m_d^2)^{1/2} - i\epsilon] ,$$

with $\alpha \equiv 2\sqrt{\eta(1+\eta)}$. While the left-hand pole causes no trouble, the right-hand one can, for certain values of $|\mathbf{k}|$ and $\cos\theta$, show up in the third quadrant as soon as $\mathbf{q}^2 > m_d(2m_N - m_d) > 0.107\ \text{fm}^{-2}$, and consequently be hit by the integration path in the Wick-rotation process. However, the residue of this first-order pole can very simply be calculated and added. Furthermore, the outgoing vertex function has poles at

$$k_0 = -\eta m_d \pm [(\mathbf{k}^2+\beta_{ab}^2+\alpha m_d|\mathbf{k}|\cos\theta + \tfrac{1}{4}\alpha^2 m_d^2)^{1/2} - i\epsilon] ,$$

whereof again the right-hand one may reach the third quadrant, viz., for $\mathbf{q}^2 \gtrsim 30\ \text{fm}^{-2}$ and $|\mathbf{k}|$, $\cos\theta$ appropriate. Also this contribution can be computed straightforwardly, although now the pole is of second order (unless $a=1, b=2$). Albeit analytically feasible, in view of the complicated expression of the integrand the residue of the double pole is computed by numerical differentiation. With all the singularities accounted for, the Wick rotation can be carried out, which now amounts to replacing k_0 by ik_4 with k_4 real. In order to achieve a satisfactory numerical stability, additional measures must be taken, as the above-described poles may come arbitrarily close to the real k_4 axis when changing quadrants. Thereto, several subtractions are performed, so as to make the integrand vanish whenever such happens. As a result, a precision of better than 1% is accomplished for the total three-dimensional numerical integration over the whole range of momentum transfers $\mathbf{q}^2$ up to 50 fm^{-2}, with a reasonable number of mesh points.

Now we are in a position to do the final computations. The nucleon form factors to be used as input are from Ref. 9, but this specific choice is of little significance, since our investigation is primarily of a comparative nature. The influence of using a different parametrization is discussed below. In order to be able to make definite statements about the relative importance of the different relativistic effects, several approximative calculations will be carried out, too. First, we reemphasize that negative-energy states are going to be neglected, which implies the restriction of the summation indices in Eq. (32) to the values 1,2, i.e., to the channels $^3S_1^+, {}^3D_1^+$. In ZT it was shown that this restraint is of little consequence, at least up to momentum transfers of 50 fm^{-2}, *provided* that the boost transformations on the EM vertex $\Gamma(q^2)$ are taken into account. Thus, we consider the following cases: (i) a purely nonrelativistic approach, denoted by NR; (ii) a minimally relativistic calculation, employing a BSLT propagator, but further completely nonrelativistic: BSLT; (iii) the so-called static approximation, which amounts to neglecting the boost on the argument of the outgoing deuteron vertex function $\phi(k')$ and on the one-particle propagator $S^{(1)}(k')$, i.e., to evaluating them at $(k_0', |\mathbf{k}'|)=(k_0, |\mathbf{k}+\frac{1}{2}\mathbf{q}|)$, but for the reason mentioned above, not on $\Gamma(q^2)$: SA; (iv) as SA, but including the boost on $S^{(1)}(k')$, while computing $\phi(k')$ and $\phi(k)$ in the resulting pole term for the SA arguments $(0, |\mathbf{k}+\frac{1}{2}\mathbf{q}|)$ and $(0, |\mathbf{k}|)$, respectively: BG; (v) as BG, but Taylor expanding $\phi(k')$ to first order about the SA value, leaving, however, the pole term unaltered. This is the approximation employed in ZT: ZT; (vi) as ZT, but also expanding $\phi(k')$ and $\phi(k)$ in the pole term to first order about the respective SA values: BT; (vii) the exact positive-energy calculation, including pole contributions from the outgoing vertex function: BS.

Since the Graz-II interaction seems to favor a D-state probability of about 5%, we first focus our attention on this case. In Fig. 1 the deviations of the predictions for the electric form factor $A(q^2)$ corresponding to the approximative calculations SA, BG, ZT, and BT are depicted, relative to the exact BS result. The static approximation clearly ceases to be reasonable from $\mathbf{q}^2 \approx 25$ fm^{-2} upwards. Remarkable is the fact that the BG approximation is considerably better than the ZT one, which demonstrates the necessity to treat the pole of the single-particle propagator on an equal footing with the remainder of the k_0 integration, viz., to apply either a zeroth- or a first-order Taylor approximation in both of these terms. This conclusion is supported by the BT curve, which deviates less than 0.6% from the BS one, up to 50 fm^{-2}. Moreover, the BT result corroborates the conjecture in ZT that the corrections due to the singularities of the outgoing vertex function are small. For even higher momentum transfers, however, the Taylor expansion breaks down, which has been verified by testing second- and third-order approximations, too.

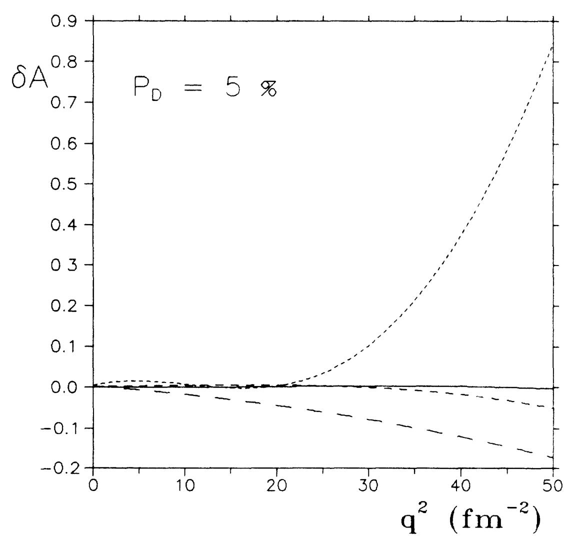

FIG. 1. Relative deviations of the electric form factor $A(q^2)$ for the cases SA ($\cdots$), BG (- - -), ZT (— —), and BT (——), with respect to the exact BS result.

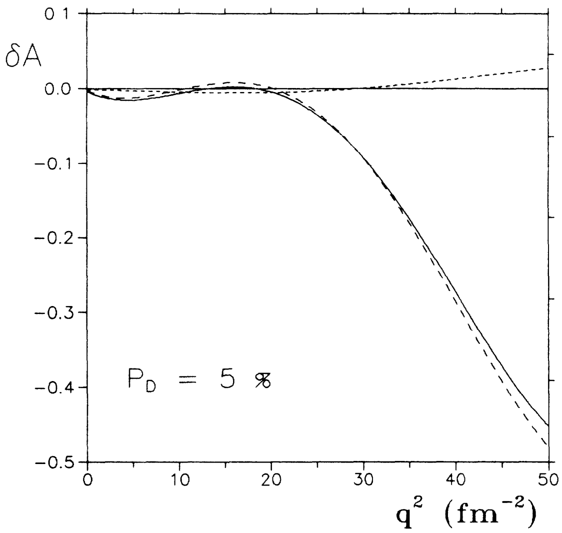

FIG. 2. As in Fig. 1, but now for the cases BS (——), BG (— — —), and their difference BV ($\cdots$), relative to SA.

In Fig. 2 the same results are depicted in a slightly different manner, namely, displaying the relative corrections to the static approximation from the boost effects, through the curves BS and BG, and their difference BV. Thus, we see that the boost on the one-particle propagator is far more important than on the vertex function (BV), namely, -49% vs $+\ 3\%$ at $\mathbf{q}^2=50$ fm^{-2}, the latter being of the same order of magnitude as the corrections due to the negative-energy states according to ZT. In order to compare different approaches with respect to relativity, we depict in Fig. 3 the same quantity for the cases BSLT, SA, and BS, relative to the NR one. While the to-

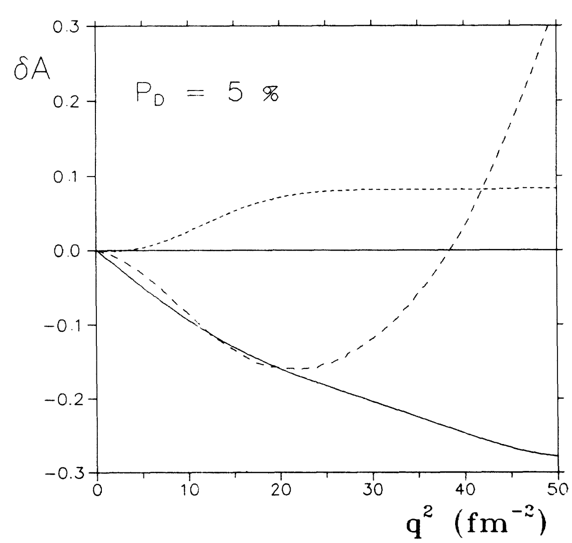

FIG. 3. As in Fig. 1 but now for the cases BSLT ($\cdots$), SA (- - -) and BS (——), relative to NR.

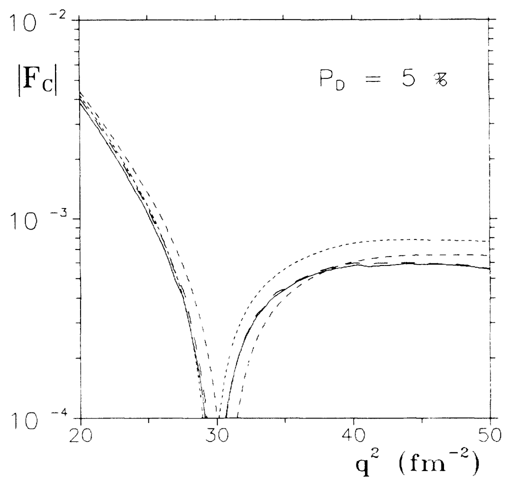

FIG. 4. Charge form factor $|F_C(q^2)|$ for the cases NR (· · ·), BSLT (- - -), SA (— —), and BS (——).

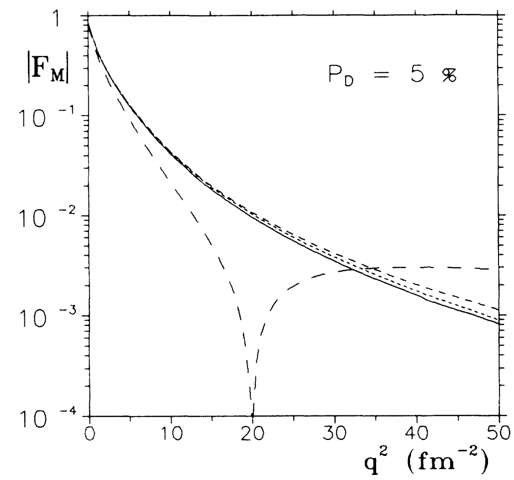

FIG. 6. Magnetic form factor $|F_M(q^2)|$ for the cases NR (· · ·), BSLT (- - -), SA (— —), and BS (——), in units of $em_d/2m_N^2$.

tal relativistic effect turns out to be not very substantial though significant, minimal relativity appears as an unreliable approximative approach. Furthermore, from Fig. 3 we see that the static approximation is similar to the NR calculation at low q^2, but deviates considerably at higher momentum transfer. This should be contrasted with the observations in ZT for the case of the OBE model.

Still for the same P_D, the charge form factor F_C corresponding to the cases NR, BSLT, SA, and BS is shown in Fig. 4, for 20 $fm^{-2} \le q^2 \le 50$ fm^{-2}. Here, relativity seems to have little influence on the position of the diffraction minimum, which, however, lies at much higher momentum transfers than, e.g., in ZT. Noteworthy is the confluence of the SA and BS curves. An analogous comparison for the quadrupole form factor F_Q yields only marginal differences among these four cases, hardly visible on a logarithmic scale.

As for the magnetic form factor $B(q^2)$, relative deviations from the BS calculation are depicted in Fig. 5, concerning the cases NR, BSLT, BG, ZT, and BT. Qualitatively, we see the same type of differences as for $A(q^2)$, though considerably larger. For instance, the BS result at 50 fm^{-2} is almost a factor of 3 larger than the ZT approximation. If we extrapolate by applying a similar correction to the OBE calculation of Ref. ZT, then their predicted magnetic form factor could turn out to lie much closer to the experimental data of Refs. 1 and 2 than expected. Besides, the SA curve has not been drawn in Fig. 5, since it would distort the graph completely. This becomes evident from Fig. 6, where F_M is shown for the approaches NR, BSLT, SA, and BS. The static ap-

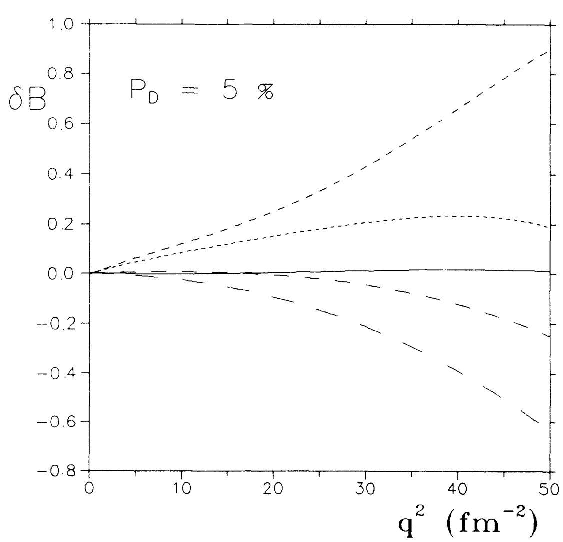

FIG. 5. Relative deviations of the magnetic form factor $B(q^2)$ for the cases NR (· · ·), BSLT (- - -), BG (— —), ZT (— —), and BT (——), with respect to the exact BS result.

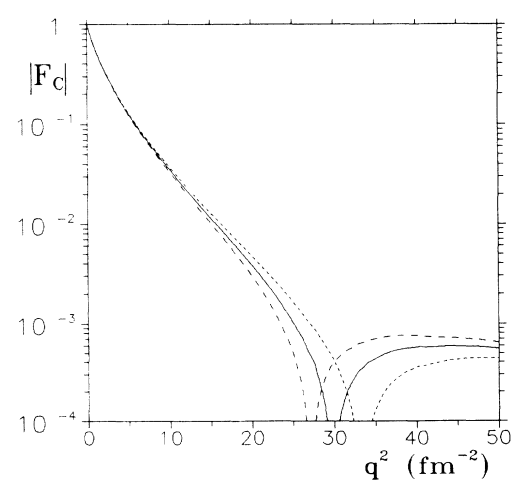

FIG. 7. Charge form factor $|F_C(q^2)|$ for the BS case with D-state probabilities of $P_D = 4\%$ (· · ·), 5% (——), and 6% (- - -).

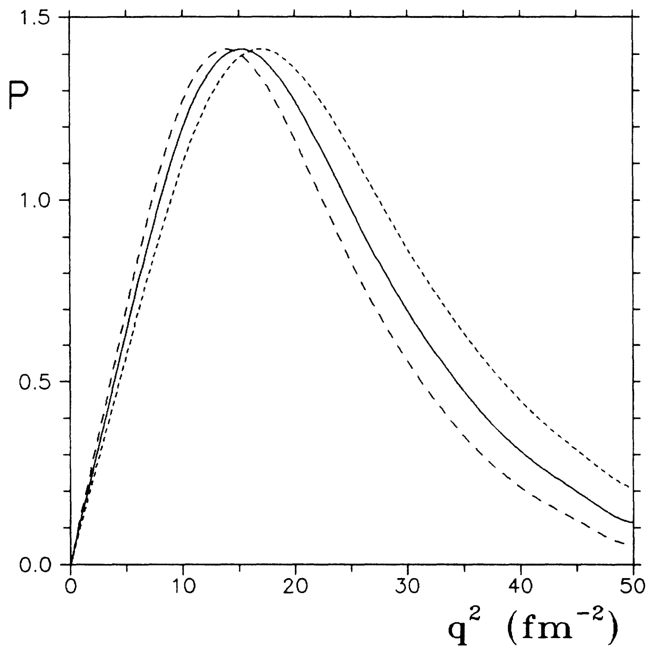

FIG. 8. As in Fig. 7, but now concerning the tensor polarization $P(q^2)$.

proximation, being the only one that produces a diffraction minimum, is completely off and thus obviously embodies the source of discrepancies in the observable $A(q^2)$ between the cases BS and SA, as we have seen above that the respective F_C and F_Q curves are very similar. An analogous phenomenon, albeit much less pronounced, can be observed in Ref. ZT, Figs. 10, 8, and 9. Next we investigate the effect of changing the D-state probability P_D.

In Fig. 7 F_C is depicted for the BS calculations with

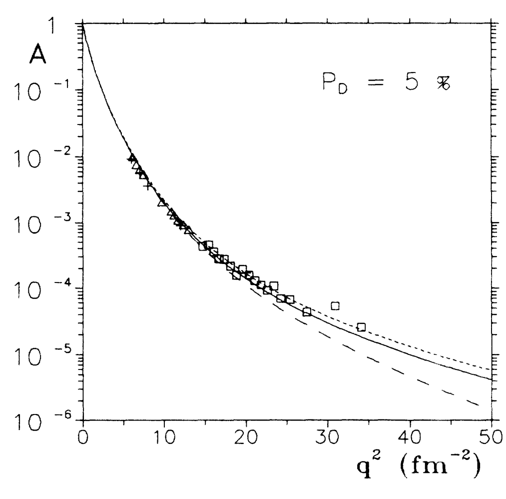

FIG. 9. Electric form factor $A(q^2)$ for the cases NR ($\cdots$) and BS (——) with nucleon form factors from Ref. 9, and for the BS case with those from Ref. 10 (— —); experimental data are from Refs. 11 (□), 12 (△), and 13 (+).

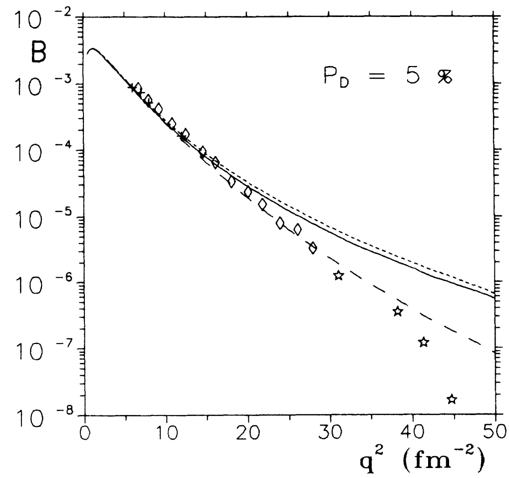

FIG. 10. As in Fig. 9, but now concerning the magnetic form factor $B(q^2)$; experimental data are from Refs. 1 (◇), 2 (☆), and 13 (+).

$P_D=4\%$, 5%, and 6%. Increasing P_D clearly moves the diffraction minimum to lower momentum transfers, although with the used separable interactions it is not possible to attain a value as low as with the OBE potentials of ZT. A similar pattern can be observed in Fig. 8, concerning the tensor polarization defined by

$$P(q^2)=\frac{4\sqrt{2}}{3}\eta\frac{F_CF_Q+\frac{1}{3}\eta F_Q^2}{F_C^2+\frac{8}{9}\eta^2F_Q^2} \ . \tag{35}$$

Here, the maximum of the curve moves inwards according as P_D increases, but not enough to produce a zero within the range of momentum transfers considered, which is clearly related to the behavior of F_C.

Finally, in Figs. 9 and 10 we show to what extent a different choice for the nucleonic form factors may affect the deuteron results, referring to Ref. 3 for a more detailed comparative study. The curves drawn, for $P_D=5\%$, are the BS predictions for $A(q^2)$ and $B(q^2)$, respectively, with the parametrizations of Refs. 9 and 10, and for comparison also the NR ones corresponding to the former choice. Hence, it becomes clear that the experimental nucleonic uncertainties are still greater than the total corrections due to relativity. Apart from that, we conclude that the used interactions are not capable of reproducing the recently measured[2] diffraction minimum in the magnetic form factor.

V. CONCLUDING REMARKS

The aim of this paper has been to study in a solvable model the various relativistic corrections to the deuteron EM form factors. The covariance of the chosen separable interactions and the gauge invariance of the associated two-body EM current, as well as the very deuteron results, guarantee that the chosen approach can be considered realistic, in spite of being purely phenomenological. Since the starting point was a nonrelativistic potential, and in order to shorten the numerical work, channels containing negative-energy states were discarded in the final calculations, in accord with observations in Ref. ZT concerning their insignificance. Thus, we obtained appreciable relativistic effects for the various form factors, of which the boost on the one-particle propagator due to recoil turned out to be by far the most important, in qualitative agreement with ZT. Furthermore, the static approximation was shown to be reasonable for the charge and quadrupole form factors, but not for the magnetic one, which is hardly surprising from a naive point of view. Still in connection with ZT, we demonstrated that an excellent approximation to the exact results, for the momentum transfers considered, can be obtained by expanding the vertex function to first order about its SA value, both in the k_0 integration and in the pole term stemming from the single-particle propagator. Limiting this procedure to the former term, as done in ZT, was found to be a worse approximation than neglecting boost effects on the vertex function completely.

ACKNOWLEDGMENTS

Part of this work was done while one of the authors (G.R.) was at the Centre de Physique Théorique, Centre National de la Recherche Scientifique, in Marseille-Luminy, and visiting the International Centre for Theoretical Physics in Trieste. Both institutions are thanked for the offered hospitality and computer facilities.

APPENDIX A: GAUGE INVARIANCE OF THE CURRENT

In this appendix we show that gauge invariance is satisfied in our separable model. We proceed in a similar fashion as in ZT, writing

$$q^{\mu}\Gamma_{\mu}^{(1)}=F_1^{(N)}\not{q}=F_1^{(N)}[S^{(1)^{-1}}(p';P')-S^{(1)^{-1}}(p;P)]\ , \tag{A1}$$

so that

$$q^{\mu}\langle P',M'|J_{\mu}^{d}|P,M\rangle\propto\int d^4p\,\bar{\phi}^{(M')}(p';P')[S(p;P)-S(p';P')]\phi^{(M)}(p;P)\ . \tag{A2}$$

Now we substitute the homogeneous BS equation once in both terms on the right-hand side and apply only in the second term a change of integration variable, viz., $\int d^4p=\int d^4(p+\frac{1}{2}q)=\int d^4p'$, whereafter the dummy prime is dropped. Thus, the expression becomes

$$\int d^4p\int d^4k[\bar{\phi}^{(M')}(k;P')S(k;P')V(k,p+\tfrac{1}{2}q)S(p;P)\phi^{(M)}(p;P)-\bar{\phi}^{(M')}(p;P')S(p;P')V(p-\tfrac{1}{2}q,k)S(k;P)\phi^{(M)}(k;P)]\ . \tag{A3}$$

Next we make use of the separability of the interaction, i.e.,

$$V(p,p')=\sum_{i,j=1}^{N}\lambda_{ij}g_i(p)\bar{g}_j(p')\ , \tag{A4}$$

where the generalized form factor g is a vector in two-particle spin and energy-spin space. Then, V satisfies the transformation law

$$V(p,p')=\Lambda^{(1)}(\mathcal{L})\Lambda^{(2)}(\mathcal{L})V(\mathcal{L}^{-1}p,\mathcal{L}'^{-1}p')\Lambda^{(1)^{-1}}(\mathcal{L}')\Lambda^{(2)^{-1}}(\mathcal{L}')\ . \tag{A5}$$

Choosing now the Breit frame, i.e., $\mathcal{L}'=\mathcal{L}^{-1}$, substituting Eqs. (A4) and (A5) into Eq. (A3), and transforming the integrand for both variables to the c.m. frame gives

$$\sum_{i,j=1}^{N}\lambda_{ij}\int d^4p\int d^4k[\bar{\phi}^{(M')}(k;P)S(k;P)g_i(k)\bar{g}_j(p+\tfrac{1}{2}\mathcal{L}^{-1}q_B)S(p;P)\phi^{(M)}(p;P)$$
$$-\bar{\phi}^{(M')}(p;P)S(p;P)g_j(p-\tfrac{1}{2}\mathcal{L}q_B)\bar{g}_i(k)S(k;P)\phi^{(M)}(k;P)]\ , \tag{A6}$$

where all cm labels have been dropped, the label B refers to the Breit frame, and where we have used the symmetry of λ_{ij} in the second term. Moreover, since $q_B=(0,\mathbf{q})$, we have $\mathcal{L}^{-1}q_B=-\mathcal{L}q_B$. Then, choosing the photon momentum along the z axis, we see from Eq. (34) that it is sufficient to consider the case $M'=M$. Finally, we evaluate Eq. (A6) on the two-particle helicity basis employed in the text. Thus, writing

$$g(p;a)=\bar{V}_{\lambda_1}^{\rho_1}(\mathbf{p})\bar{V}_{\lambda_2}^{\rho_2}(\mathbf{p})g(p)$$

and

$$\bar{g}(p;a)=\bar{g}(p)V_{\lambda_1}^{\rho_1}(\mathbf{p})V_{\lambda_2}^{\rho_2}(\mathbf{p})\ , \tag{A7}$$

with $\bar{g}(p;a)=-g(p;a)$, and where a is shorthand for $\lambda_1,\lambda_2,\rho_1,\rho_2$, we get, omitting the references to P and M,

$$\sum_{i,j=1}^{N}\lambda_{ij}\sum_{a,b}\int d^4p\int d^4k[\phi(k;a)S(k;a)g_i(k;a)Z(\mathbf{p},\sigma;a,b)g_j(\sigma;b)S(p;b)\phi(p;b)$$
$$-\phi(p;b)S(p;b)g_j(\sigma;b)Z(\sigma,\mathbf{p};b,a)g_i(k;a)S(k;a)\phi(k;a)]\ , \tag{A8}$$

where $\sigma\equiv p-\frac{1}{2}\mathcal{L}q_B$ and $Z(\mathbf{p},\sigma;a,b)\equiv V_{\lambda_1}^{\rho_1\dagger}(\mathbf{p})V_{\lambda_2}^{\rho_2\dagger}(\mathbf{p})V_{\lambda_1'}^{\rho_1'}(\sigma)V_{\lambda_2'}^{\rho_2'}(\sigma)$. Note that the two-body Green's function is diagonal in this basis. Now, $Z(\sigma,\mathbf{p};b,a)=Z^{\dagger}(\mathbf{p},\sigma;b,a)=Z^{*}(\mathbf{p},\sigma;a,b)$, whence, as

$$\int_0^{2\pi}d\varphi\, Z(\mathbf{p},\sigma;a,b)=\int_0^{2\pi}d(-\varphi)Z(\mathbf{p},\sigma;a,b)=\int_0^{2\pi}d\varphi\, Z^{*}(\mathbf{p},\sigma;a,b)\ , \tag{A9}$$

expression (A8) vanishes identically. The fact that we have chosen a special frame and a specific direction for the photon momentum is irrelevant, since the evaluated quantity is a Lorentz scalar.

APPENDIX B: MATRIX ELEMENTS OF THE ELECTROMAGNETIC OPERATOR

In this appendix we give the explicit expressions for the matrix elements of the electromagnetic operator corresponding to positive-energy states. Defining $\Gamma_5^{(1)}q\equiv i\gamma^1\gamma^2\Gamma_1^{(1)}(q)$, and [cf. Eq. (33)]

$$\begin{aligned}\tilde{\Gamma}_\mu^{(1)}(q;\lambda_1'\lambda_2',\lambda_1\lambda_2)&=\bar{V}^{+}_{\lambda_1'}(\mathbf{k}')V^{+\dagger}_{\lambda_2'}(\mathbf{k}')\Lambda^{(1)}(\mathcal{L})\Gamma^{(1)}_\mu(q)\Lambda^{(1)}(\mathcal{L})[\Lambda^{(2)}(\mathcal{L})]^2V^{+}_{\lambda_1}(\mathbf{k})V^{+}_{\lambda_2}(\mathbf{k})\\&=\bar{V}^{+}_{\lambda_1'}(\mathbf{k}')\Lambda^{(1)}(\mathcal{L})\Gamma^{(1)}_\mu(q)\Lambda^{(1)}(\mathcal{L})V^{+}_{\lambda_1}(\mathbf{k})V^{+\dagger}_{\lambda_2'}(\mathbf{k}')[\Lambda^{(2)}(\mathcal{L})]^2V^{+}_{\lambda_2}(\mathbf{k})\\&\equiv\tilde{\Gamma}^{(1)}_\mu(q;\lambda_1',\lambda_1)\tilde{W}^{(2)}(q;\lambda_2',\lambda_2)\ ,\end{aligned} \tag{B1}$$

we obtain with the aid of REDUCE the following results:

$$\tilde{W}^{(2)}(q;+,+)=\frac{1}{\mathcal{E}}\left\{\sqrt{1+\eta}[(E_k+m_N)(E_{k'}+m_N)+|\mathbf{k}||\mathbf{k}'|]\cos\frac{\theta-\theta'}{2}+\sqrt{\eta}[|\mathbf{k}|(E_{k'}+m_N)+|\mathbf{k}'|(E_k+m_N)]\cos\frac{\theta+\theta'}{2}\right\}\ , \tag{B2}$$

$$\tilde{W}^{(2)}(q;+,-)=\frac{1}{\mathcal{E}}\left\{-\sqrt{1+\eta}[(E_k+m_N)(E_{k'}+m_N)-|\mathbf{k}||\mathbf{k}'|]\sin\frac{\theta-\theta'}{2}+\sqrt{\eta}[|\mathbf{k}|(E_{k'}+m_N)-|\mathbf{k}'|(E_k+m_N)]\sin\frac{\theta+\theta'}{2}\right\};$$

$$\begin{aligned}\tilde{\Gamma}_0^{(1)}(q;+,+)=\frac{1}{\mathcal{E}}\Bigg[&\left\{[(E_k+m_N)(E_{k'}+m_N)+|\mathbf{k}||\mathbf{k}'|]F_1^{(N)}-\eta\frac{m_d}{m_N}[(E_k+m_N)(E_{k'}+m_N)-|\mathbf{k}||\mathbf{k}'|]F_2^{(N)}\right\}\cos\frac{\theta-\theta'}{2}\\&+\sqrt{\eta(1+\eta)}\frac{m_d}{m_N}[|\mathbf{k}|(E_{k'}+m_N)-|\mathbf{k}'|(E_k+m_N)]F_2^{(N)}\cos\frac{\theta+\theta'}{2}\Bigg]\ ,\end{aligned}$$
$$\tag{B3}$$
$$\begin{aligned}\tilde{\Gamma}_0^{(1)}(q;+,-)=\frac{1}{\mathcal{E}}\Bigg[&\left\{[-(E_k+m_N)(E_{k'}+m_N)+|\mathbf{k}||\mathbf{k}'|]F_1^{(N)}+\eta\frac{m_d}{m_N}[(E_k+m_N)(E_{k'}+m_N)+|\mathbf{k}||\mathbf{k}'|]F_2^{(N)}\right\}\sin\frac{\theta-\theta'}{2}\\&+\sqrt{\eta(1+\eta)}\frac{m_d}{m_N}[|\mathbf{k}|(E_{k'}+m_n)+|\mathbf{k}'|(E_k+m_N)]F_2^{(N)}\sin\frac{\theta+\theta'}{2}\Bigg]\ ,\end{aligned}$$

$$\begin{aligned}\tilde{\Gamma}_1^{(1)}(q;+,+)=\frac{1}{\mathcal{E}}\Bigg[&-\sqrt{\eta}\left\{[(E_k+m_N)(E_{k'}+m_N)+|\mathbf{k}||\mathbf{k}'|]F_1^{(N)}+\frac{m_d}{m_N}[(E_k+m_N)(E_{k'}+m_N)-|\mathbf{k}||\mathbf{k}'|]F_2^{(N)}\right\}\sin\frac{\theta-\theta'}{2}\\&-\sqrt{\eta(1+\eta)}[|\mathbf{k}|(E_{k'}+m_N)+|\mathbf{k}'|(E_k+m_N)]F_1^{(N)}\sin\frac{\theta+\theta'}{2}\Bigg]\ ,\end{aligned}$$
$$\tag{B4}$$
$$\begin{aligned}\tilde{\Gamma}_1^{(1)}(q;+,-)=\frac{1}{\mathcal{E}}\Bigg[&-\sqrt{\eta}\left\{[(E_k+m_N)(E_{k'}+m_N)-|\mathbf{k}||\mathbf{k}|']F_1^{(N)}+\frac{m_d}{m_N}[(E_k+m_N)(E_{k'}+m_N)+|\mathbf{k}||\mathbf{k}'|]F_2^{(N)}\right\}\cos\frac{\theta-\theta'}{2}\\&+\sqrt{\eta(1+\eta)}[|\mathbf{k}|(E_{k'}+m_N)-|\mathbf{k}'|(E_k+m_N)]F_1^{(N)}\cos\frac{\theta+\theta'}{2}\Bigg]\ ,\end{aligned}$$

$$\tilde{\Gamma}_5^{(1)}(q;+,+)=\frac{1}{\mathcal{E}}\Bigg[\sqrt{\eta}\left\{[(E_k+m_N)(E_{k'}+m_N)+|\mathbf{k}||\mathbf{k}'|]F_1^{(N)}+\frac{m_d}{m_N}[(E_k+m_N)(E_{k'}+m_N)-|\mathbf{k}||\mathbf{k}'|]F_2^{(N)}\right\}\sin\frac{\theta+\theta'}{2}$$

$$+\sqrt{\eta(1+\eta)}[|\mathbf{k}|(E_{k'}+m_N)+|\mathbf{k}'|(E_k+m_N)]F_1^{(N)}\sin\frac{\theta-\theta'}{2}\Bigg] ,$$

$$\tilde{\Gamma}_5^{(1)}(q;+,-)=\frac{1}{\mathcal{E}}\left[\sqrt{\eta}\left\{[(E_k+m_N)(E_{k'}+m_N)-|\mathbf{k}||\mathbf{k}'|]F_1^{(N)}+\frac{m_d}{m_N}[(E_k+m_N)(E_{k'}+m_N)+|\mathbf{k}||\mathbf{k}'|]F_2^{(N)}\right\}\cos\frac{\theta+\theta'}{2}\right.$$
$$\left.-\sqrt{\eta(1+\eta)}[|\mathbf{k}|(E_{k'}+m_N)-|\mathbf{k}'|(E_k+m_N)]F_1^{(N)}\cos\frac{\theta-\theta'}{2}\right] . \tag{B5}$$

Here, $\mathcal{E}\equiv 2\sqrt{E_kE_{k'}(E_k+m_N)(E_{k'}+m_N)}$. The remaining terms can easily be obtained through the following symmetry properties:

$$\tilde{W}^{(2)}(q;-,+)=-\tilde{W}^{(2)}(q;+,-),\ \tilde{W}^{(2)}(q;-,-)=\tilde{W}^{(2)}(q;+,+) ,$$
$$\tilde{\Gamma}_\mu^{(1)}(q;-,+)=-\tilde{\Gamma}_\mu^{(1)}(q;+,-),\ \tilde{\Gamma}_\mu^{(1)}(q;-,-)=\tilde{\Gamma}_\mu^{(1)}(q;+,+)\quad \text{for } \mu=0,1 , \tag{B6}$$
$$\tilde{\Gamma}_5^{(1)}(q;-,+)=\tilde{\Gamma}_5^{(1)}(q;+,-),\ \tilde{\Gamma}_5^{(1)}(q;-,-)=-\tilde{\Gamma}_5^{(1)}(q;+,+) .$$

[1]S. Auffret *et al.*, Phys. Rev. Lett. **54**, 649 (1985).

[2]R. G. Arnold *et al.*, Phys. Rev. Lett. **58**, 1723 (1987).

[3]R. G. Arnold, C. E. Carlson, and F. Gross, Phys. Rev. C **21**, 1426 (1980).

[4]M. J. Zuilhof and J. A. Tjon, Phys. Rev. C **22**, 2369 (1980); M. J. Zuilhof, Ph.D. thesis, University of Utrecht, 1981 (unpublished).

[5]G. Rupp and J. A. Tjon (unpublished).

[6]L. Mathelitsch, W. Plessas, and W. Schweiger, Phys. Rev. C **26**, 65 (1982).

[7]R. Blankenbeckler and R. Sugar, Phys. Rev. **142**, 1051 (1966); A. A. Logunov and A. N. Tavkhelidze, Nuovo Cimento **29**, 380 (1963).

[8]G. Rupp and J. A. Tjon, Phys. Rev. C **37**, 1729 (1988).

[9]T. Janssens, R. Hofstadter, E. B. Hughes, and M. R. Yearian, Phys. Rev. **142**, 922 (1966); F. Iachello, A. D. Jackson, and A. Lande, Phys. Lett. **43B**, 191 (1973).

[10]G. Höhler, E. Pietarinen, I. Sabba-Stefanescu, F. Borkowski, G. G. Simon, V. H. Walther, and R. D. Wendling, Nucl. Phys. **B114**, 505 (1976).

[11]J. E. Elias, J. I. Friedman, G. C. Hartmann, M. W. Kendall, P. N. Kirk, M. R. Sogard, L. P. Van Speybroeck, and J. K. De Pagter, Phys. Rev. **177**, 2075 (1969).

[12]S. Galster, M. Klein, J. Moritz, K. M. Schmidt, D. Wegener, and J. Bleckwenn, Nucl. Phys. **B32**, 221 (1971).

[13]C. D. Buchanan and M. R. Yearian, Phys. Rev. Lett. **15**, 303 (1965).